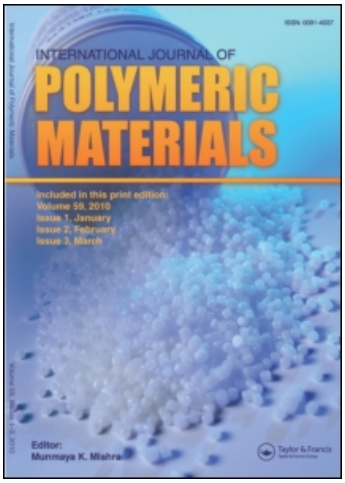

International Journal of Polymeric Materials
Publication details, including instructions for authors and subscription information:
http://www.informaworld.com/smpp/title~content=t713647664

Slow Crack Growth and Molecular Mobility in Commercial Gas Pipe Resins

J. J. Lear[a]; P. H. Geil[a]
[a] Polymer Division, Department of Materials Science and Engineering, University of Illinois at Urbana-Champaign, Urbana, IL

To cite this Article Lear, J. J. and Geil, P. H.(1991) 'Slow Crack Growth and Molecular Mobility in Commercial Gas Pipe Resins', International Journal of Polymeric Materials, 15: 3, 147 — 170
To link to this Article: DOI: 10.1080/00914039108041081
URL: http://dx.doi.org/10.1080/00914039108041081

Intern. J. Polymeric Mater., 1991, Vol. 15, pp. 147–170
Reprints available directly from the publisher
Photocopying permitted by license only

Printed in the United Kingdom

Slow Crack Growth and Molecular Mobility in Commercial Gas Pipe Resins

J. J. LEAR and P. H. GEIL

Polymer Division, Department of Materials Science and Engineering, University of Illinois at Urbana-Champaign, 1304 West Green Street, Urbana, IL 61801

(Received April 3, 1991)

Fundamentals of crack growth were studied in polyethylene copolymers used in distribution piping of natural gas. The effect of comonomers is significant despite very low concentrations. The growth of the craze is by fibrillation at the crack tip. The molecular mobility was studied by dynamic mechanical properties as well as by small angle x-ray scattering measurements of the changes in long period with annealing time and temperature. It was found that molecular mobility in these gas pipe resins is significantly less than that seen in HDPE. This greatly reduced molecular mobility seems to contribute to the increased resistance to slow crack growth of these resins.

KEY WORDS Polyethylene, copolymers, crack growth

INTRODUCTION

Since the introduction of polyethylene (PE) pipe in the late sixties and early seventies for use in natural gas distribution, nearly one billion feet of various grades have been installed in North America.[1] Now more than 80% of all pipe installed for natural gas distribution is made of PE, and this percentage is increasing annually.[2] The PE resins currently used in the natural gas industry are ethylene and α-olefin copolymers. The α-olefin is generally either 1-hexene or 1-octene, resulting in side branches of 4 or 6 carbons, respectively. It is produced by a process similar to that used in the manufacture of linear low density polyethylene (LLDPE) which most often uses 1-butene as its comonomer in amounts that result in 50–100 branches per 1000 backbone carbons. A significant difference between LLDPE and the PE resins used for natural gas pipes is the number of side branches. In natural gas pipe resins the number of branches is kept relatively low, somewhere in the range of 3–10 branches per 1000 backbone carbons, such that the resulting density is between 0.926 and 0.940 gm/cc. Therefore, these resins fall within the medium to high density range, significantly above the densities for the resins commonly called LLDPE which are used in packaging film applications.

Ease of installation was one of the primary reasons for the switch from metal pipes. Polyethylene pipes and fittings may be thermally fused for secure joints. At

the surfaces of the two components to be joined, some of the polymer is melted and fused together, forming one continuous piece of material. A properly fused joint will be as strong as the surrounding material. Furthermore, the joint is accomplished without chemicals or adhesives and its security does not rely on additional parts, such as metal couplers, which must be left in place. Unfortunately, occasional and unexpected field failure of the PE pipe have been reported.[3]

Due to the relatively recent use of PE material in the gas industry, only limited information on the failure behavior of PE pipe is currently available. Crack growth in commercial piping materials and the influence that molecular mobility might have on crack growth will be discussed in this paper. The long range goal is to be able to rank various pipe resins as to their expected lifetime by use of a theoretically and experimentally sound accelerated test. A complementary theoretical study was conducted by F. G. Yuan and S. S. Wang.[4]

Slow crack growth, the dominant mode of field failures for PE piping systems, other than for weld failures due to improper thermal joining,[5] was studied using compact tension samples. The extent of the ability to resist this type of failure dictates the ultimate service life of a given PE material. These failures generally occur under low-loads and after long periods of time. Initially, slow crack growth seems unlikely because, under long-term loading conditions near room temperature, PE normally exhibits creep-type deformation with ductile failure, but field failures by slow crack growth have been commonly reported.[5]

Slow crack growth has been termed brittle in the literature[6,7] because of the lack of any visible macroscopic ductility on the fracture surface. Impact failures are also termed brittle; however, these two failure modes are fundamentally different from each other. Although the fracture surfaces for both types of failure appear visibly smooth to the eye, on a microscopic level impact failure surfaces generated at room temperature appear "flaky." This has been attributed to microscopic cracks branching from the main fracture crack during impact.[8] In contrast, slow crack growth fractures have a fibrous texture on a microscopic level.[9] Another important difference is that impact failures in PE tend to occur at lower temperatures whereas the tendency for slow crack growth to occur increases with increasing temperature. Additionally, impact failure displays crack growth rates close to the speed of sound, while slow crack growth is characterized by a crack which propagates over a time span of a few days to several years. The rate at which these cracks propagate contributes to making them difficult to study. This paper will describe our microscopic observations of the mechanism of slow crack growth and structure of the resulting failure surface for several PE resins.

It is suspected that molecular mobility influences the failure mode and crack growth rates of these pipe resins. For example, creep rupture tests, which measure the time to failure of uniaxially loaded tensile bars at various loads, show a surprising effect, a knee in the curve, which is not seen in common creep tests. In these experiments the typical creep rupture curve displays a shallow sloped region followed by a more steeply sloped region [e.g., 10]. Generally, ductile-type failure occurs in the shallow sloped initial region of the curve, which corresponds to relatively high stress levels and short failure times, i.e. large scale deformation. In the more steeply sloped latter region of the creep rupture curve, which corresponds

to lower stress levels and longer failure times, "brittle"-type or slow crack growth failure occurs. The point where the slope changes, the knee in the curve, can be characterized as a type of ductile-brittle transition. It occurs at lower stresses as the test temperature is increased. The stresses can be significantly below the macroscopic yield point. Creep rupture tests conducted on PE water pipe,[10] to determine safe, usable lifetimes and minimum pipe wall thickness, used this knee to rank pipe material and predict long term behavior. The basis of the research reported here was our suggestion that the onset of molecular motion in the crystalline regions causes this transition of the failure surfaces from ductile to brittle behavior at the knee of creep rupture curves. At the lower stress level, the time to failure is long enough to allow many of the tie molecules to slip out of the crystalline regions resulting in the material failing with only localized macroscopic deformation in a "brittle"-type manner. Conversely, at higher stress levels and shorter times, the tie molecules cannot slip out of the crystalline regions resulting in large scale ductile deformation and a corresponding destruction and reformation of the crystalline regions similar to that occurring in normal drawing. The molecular origin of the knee would thus be expected to be related to the slow crack growth process seen in gas pipe resins.

The potential relationship between the brittle-ductile transition of the creep rupture curve and one of the components of the α-relaxation process, as observed in dynamic mechanical spectra, was investigated in our work. Takayanagi and Matsuo[11] have probably done the most extensive work on characterizing the α-relaxation. In investigating the crystalline relaxations of a high density (linear) polyethylene (HDPE, Marlex 50, similar to Marlex 6050) using a direct reading Rheovibron DDV-II dynamic viscoelastometer with bulk polymer films and single crystal mats of varying thermal history, three relaxations were found. The lowest temperature peak, α_c', characteristic of annealed single crystals and bulk crystallized samples only, was seen between 40 and 70°C. The peak shifts to higher temperatures as the annealing temperature is raised. From the fact that the α_c' absorption could only be found in the annealed single crystals and bulk crystallized samples, this absorption was associated with a mosaic block structure which Takayanagi and Matsuo propose is induced by annealing or crystallizing from the melt. They suggest the possibility that internal friction in the regions between mosaic blocks may cause the energy absorption involved although, at present, there is no direct evidence of a mosaic structure in PE.

At a temperature usually between 80 and 100°C, always higher than the α_c' peak, another relaxation, α_c, is seen. Both the intensity and temperature of this relaxation increase with increasing long period of isothermally crystallized samples. However, if the long period was increased by annealing, the intensity of this second relaxation decreases and the temperature increases. These findings were interpreted in terms of this relaxation being due to segmental motions involving defects in the crystalline portions of the mosaic blocks.

A third peak (α_f), occurring on the high temperature side of the α_c absorption and most noticeable at low frequencies, ~3.5 Hz, appears between 90 and 110°C. Its absorption temperature increases with long period. The α_f relaxation occurs at about the same temperature at which the long period of this material begins to

increase with annealing and is not reproducible (i.e. cannot be seen on the second run of the same sample if tested over the same temperature range). These facts were interpreted as meaning that the α_f relaxation is associated with irreversible structural changes of the virgin crystal, i.e. increases in fold period. It is the α_c and α_f relaxation which are of primary interest to our study since they are related to the motion of molecules in the crystalline regions. In addition to dynamic mechanical measurements, small angle x-ray studies (SAXS) were conducted to also measure molecular mobility. The change in long period versus time and versus temperature of annealing can be measured by SAXS to give an indication of chain mobility within the crystalline regions. Chains with reduced mobility (i.e. those containing side branching) will require more annealing time or higher annealing temperatures to achieve any thickening of the lamella structure.

EXPERIMENTAL

Materials

Several PE resins were studied, Marlex 400 and 8600, both pipe resins, Marlex 6050 and 6015, both HDPE, and Dowlex 2028, a LLDPE. Their characteristics are described in Table I.

Compact tension test

Compact tension (CT) samples following the ASTM E399 standard were used to study craze/crack development and the plastic deformation zone generated during craze/crack growth. The specimens measured one inch square and one quarter of an inch thick, with one-eighth inch diameter holes for the loading pins. They were cut from compression molded plaques made from pellets. The molding pellets were heated in the press for 15 minutes under heat only at 165°C and then enough pressure was applied to adequately close the entire assembly which was heated another 15 minutes. To aid in removal of any irregularities caused by sample

TABLE I

Physical properties of polyethylene resins

Properties	*Marlex 400	*Marlex 8600	*Marlex 6015	Marlex 6050	Dowlex**
Comonomer	1-Hexene	1-Hexene	none	none	1-Octene
Density, g/cc	0.950	0.957	0.96	0.96	0.94
Melt Index, g/10 min	0.25	1.5	1.5	5.0	4.0
ESCR, F_{50}, hrs	>1000	>5000	10	1	N/A

*Trademark of the Phillips 66 Company.
**Trademark of Dow Chemical Company.

preparation, a jig was used to allow reproducible placement of the pin holes used for loading and the initial notch. The initial notch was started with a band saw and then sharpened by pushing a razor blade into the sample a short distance after the sample had been cooled in liquid nitrogen for 30 minutes. Figure 1a is a micrograph of the razor blade notch as observed on the surface of an untested sample; it shows a single crack. The large square groove behind the razor blade notch is from the band saw cut. Figure 1b is a higher magnification scanning electron microscope (SEM) photo of the crack tip displaying its sharpness. Following notching, the samples were drawn at room temperature, at 0.25 inches per minute in a screw driven MTS unit, until a crack opening displacement (COD) of one-tenth of an inch was reached. The sample's notch was then held open by a wedge in order to allow further observations. In order to allow comparisons among different speci-

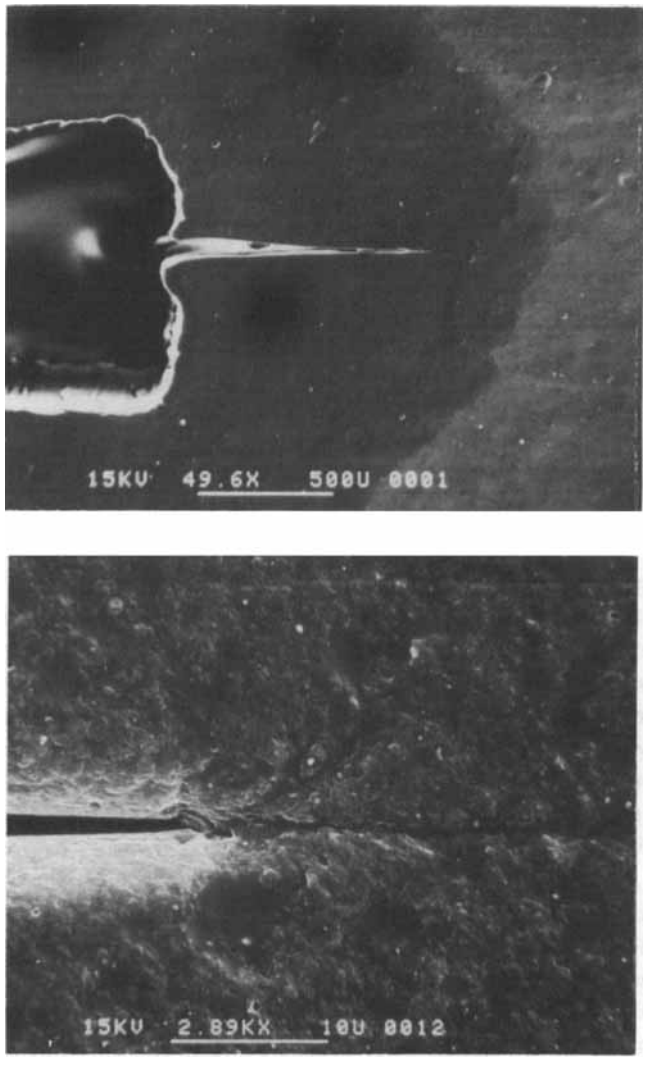

FIGURE 1 a) Razor blade notch in untested sample, b) higher magnification.

mens and materials the reproducibility of the length of the notch is critical because the CT samples were all pulled to the same COD.

Since the thermal conductivity of PE is low and the CT specimens were made from molded plaques 0.25 inches thick, the cooling rate was expected to have little effect on the morphology of the sample. Sample cooling rates were measured by inserting a thermocouple in between two sheets, half the thickness of the final piece and pressing the two together. Figure 2 is the cooling curve from the center of a sample cooled by water quenching in the hot press. Since there is no significant large scale molecular motion below about 80°C, the α-relaxation temperature, the rate of cooling below this point is unimportant. As can be seen, the interior of the plaque requires more than 6 minutes to reach 80°C, which is a relatively slow cooling rate. Most of the crystallization occurs in the plateau region at about 122°C. Because of this fact, the cooling rate is not expected to affect the bulk properties of molded plaques and was not varied in these experiments. Although the cooling rate had little effect on the sample's morphology, it was found that slow cooling caused considerable surface oxidation. When cooled in the press by turning off the heat, only, it takes almost 3 hours for the sample to cool to 80°C. Therefore all molded plaques used to make CT samples for use in this study were water cooled in the press.

Scanning electron microscopy (SEM)

The samples were observed in an ISI 130 SEM at an accelerating voltage of 15 kV after coating with Au-Pd. SEM was chosen because of its large depth of field, about 200 to 300 times greater than optical microscopy at the magnification required. The sample was not tilted, as is often done in SEM, in order to preserve proper perspective. In order to allow observation of the interior regions of a CT sample after being drawn, the wedged open notch was filled with a room temperature curing epoxy to maintain the crack opening during sectioning. The sample was then sectioned in half parallel to its large face by controlled slow advancement of a fresh razor blade in a direction normal to the crack growth direction. This sectioning caused significant deformation making observation of the as-cut surface impossible. Therefore, all sectioned surfaces were etched following a modification of Bassett's $KMnO_4$ technique[12] described by Rybnikar.[13] Initially the sample was etched for 1 hour in a solution containing 5 percent by weight of $KMnO_4$ dissolved in H_3PO_4. The etching was carried out in an ultrasonic bath to ensure good mixing. The sample was glued to a microscope slide with epoxy in order to prevent it from floating during etching. After etching, each sample was washed in running water for 30 minutes, rinsed for 15 minutes in H_2O_2 to remove any MnO_2 deposits, soaked in distilled water for 15 minutes and finally soaked in acetone for 15 minutes (this last step was found later to be unnecessary). The soaking and rinsing were also performed in an ultrasonic bath. This initial etching was then followed by a milder, 1% concentration, short duration (15 minutes) etch, followed by the same washing routine, to remove any residue left by the stronger initial etching.

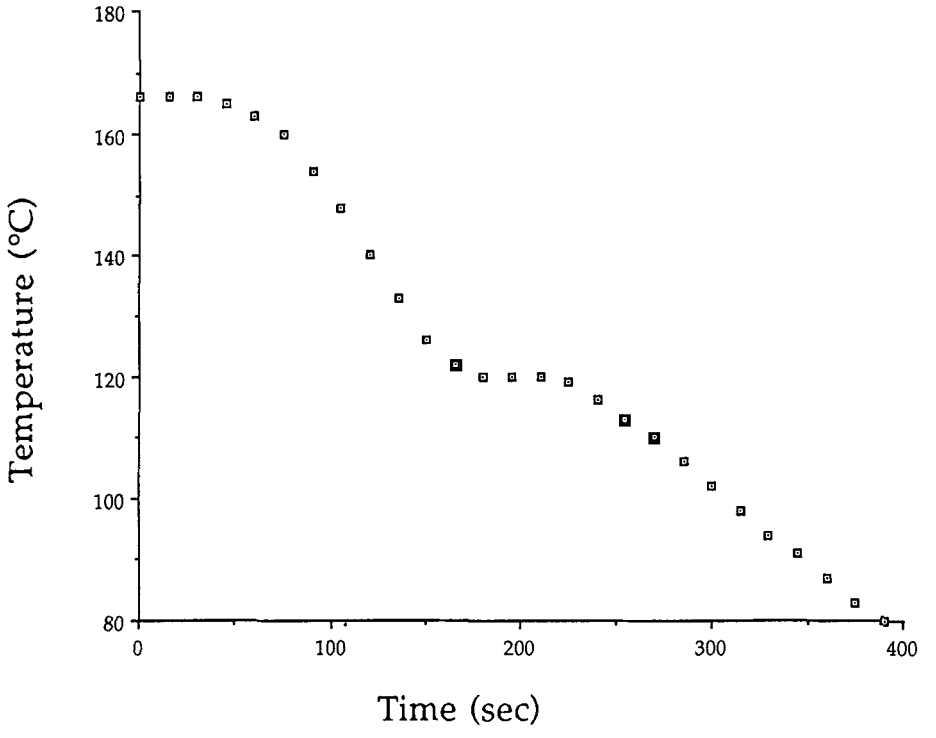

FIGURE 2 Cooling curve from the center of a PE sample cooled by water quenching in the press.

Transmission electron microscopy (TEM)

Observations were made on a JEOL 100C TEM at 100 kV using standard single stage Pt-C replicas in order to have sufficient resolution. If the surface to be examined had to be first sectioned, it was etched as described above, then platinum-carbon shadowed at 30° to give contrast to the replica when observed in the electron beam by transmission. The Pt-C coating was stripped off the specimen after a 5% aqueous solution of polyacrylic acid (PAA) had dried for 24 hours. The PAA/Pt-C sandwich was then carbon coated to provide a continuous layer necessary to hold the replica together when the PAA was later removed by soaking in water.

Dynamical mechanical measurements

The dynamic mechanical spectra (E' and E'') were measured in tension-tension mode with a Rheometrics System IV Dynamic Mechanical Spectrometer at 1 Hz and 0.2% maximum strain with a slight pretension, taking measurements at 5°C increments. Samples of various thermal histories were cut into a rectangular shape with dimensions approximately 2.5 inches long, 0.5 of an inch wide and 0.029 of an inch thick for testing.

Differential scanning calorimetry (DSC) analysis

The crystallinity of PE samples of varying thermal histories, with an average sample weight of 1.5 mg, were measured using a Perkin-Elmer DSC-4. A heating rate of

20°C was chosen for most studies. Crystallinity was determined by comparing the heat of melting, ΔH_m, of a sample to that of a 100% crystalline sample, assuming a value of 65.9 cal/gram[14] for ΔH_m of a 100% crystalline sample.

Wide angle x-ray scattering (WAXS) measurements

Measurements were made over the range of 10° to 40° 2θ with copper K_α radiation using a Scintag diffractometer in reflection mode at room temperature. The degree of crystallinity was determined by dividing the area under the diffraction curve attributed to crystalline diffraction by the total area. A baseline was drawn in to differentiate the contribution from crystalline and amorphous diffraction.

Small angle x-ray scattering (SAXS) measurements

Long period measurements were made using a pinhole collimated SAXS unit with a camera length of 1040 mm and a Rigaku copper rotating anode unit set at 40 kV and 225 mA. A 4096 channel, position sensitive proportional counter made by Technology for Energy Corporation was used to detect the intensity of the scattered radiation. Thin samples were cut and stacked together until a thickness of about one eighth of an inch was achieved in order to provide enough scattered intensity to make measurements possible with 30 minute data collection times.

RESULTS AND DISCUSSION

Slow crack growth

In order to study slow crack growth and to rank various resins with respect to their expected lifetimes, suitable test conditions and specimen geometry had to be de-

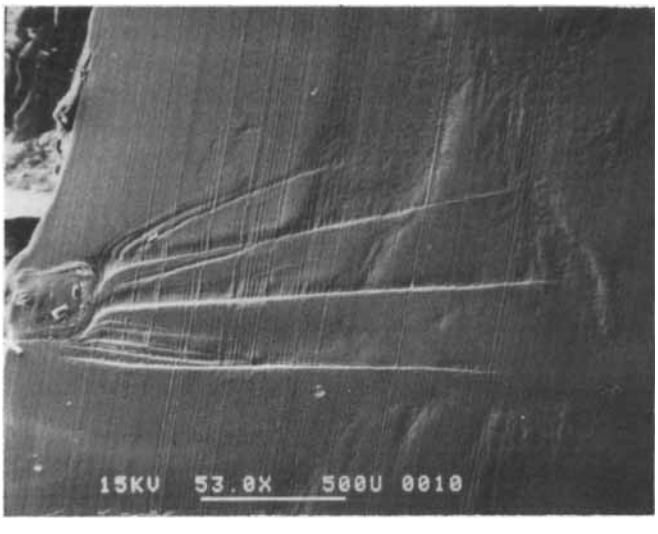

FIGURE 3 SEM micrograph of Marlex 400 interior surface as-sectioned, without etching.

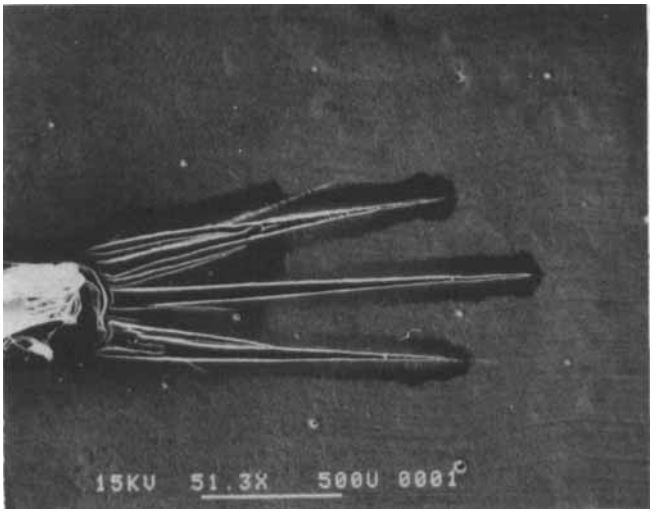

FIGURE 4 Etched interior surface of Marlex 400 drawn in air.

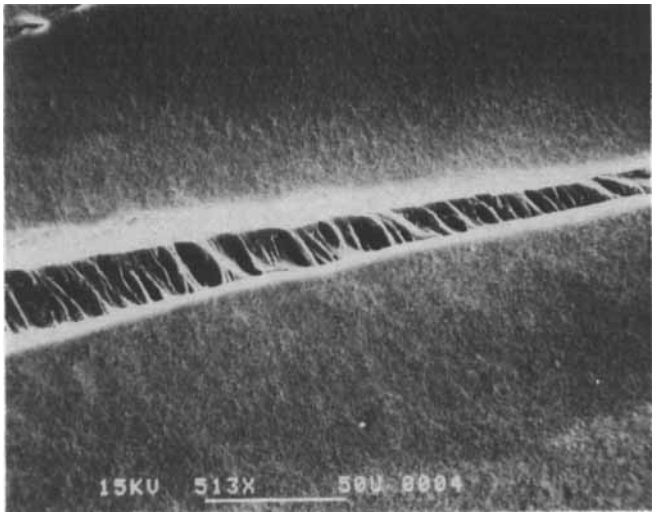

FIGURE 5 SEM micrograph near the crack tip of Marlex 400 sample drawn in air.

termined. Consideration of how to prepare suitable specimens for in-situ visual observations was a major concern. Two test geometries basic to fracture mechanic studies have appeared frequently in the literature, single edge notch (SEN)[15,16] and double edge notch (DEN) samples.[17,18] Both tests are done by tensile loading (Mode I) where the crack surfaces move directly apart. In the SEN specimens a single surface notch is usually made across the entire sample width while DEN specimens contain two notches, one at each side of the sample, across the sample's thickness. A slight variation to the DEN geometry, used on actual PE pipe,[5,19] contains a total of four notches. In this test, a ring is cut from the pipe preserving all the

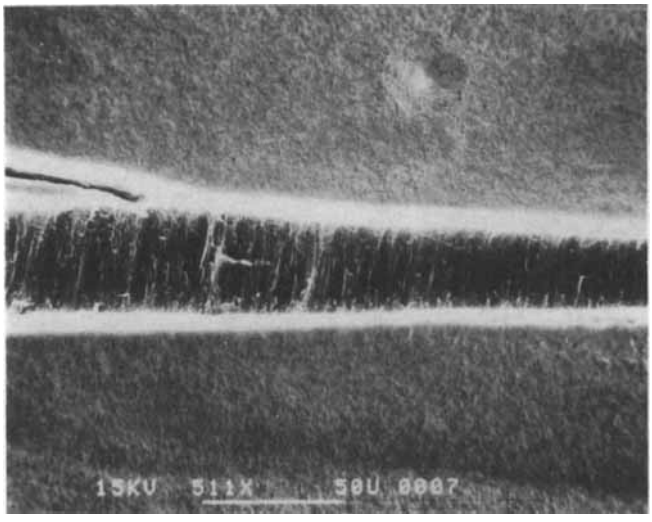

FIGURE 6 SEM micrograph of a Marlex 400 sample drawn in air showing the area near the base of the crack.

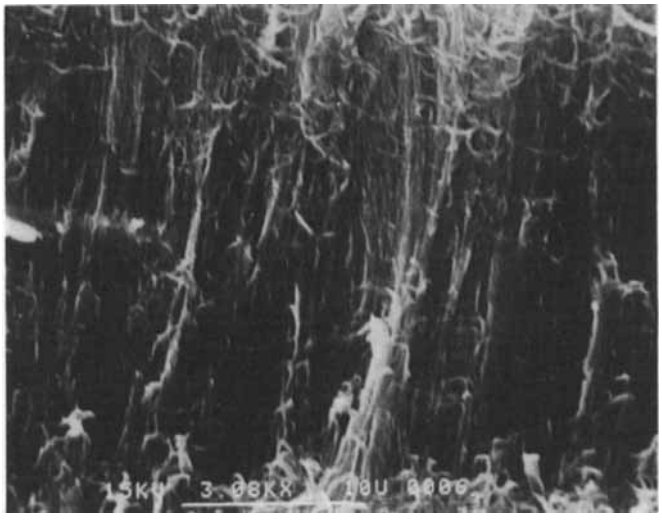

FIGURE 7 Higher magnification, SEM micrograph of a Marlex 400 sample drawn in air showing the area near the base of the crack.

processing history. The ring is then axially notched on both the interior and exterior walls at points 180° across from each other. The ring is then placed in a split-ring fixture and held under a constant load.

A limitation to these tests is their inability to isolate the effect of a resin's yield stress versus modulus. For example, in a constant strain test, HDPE generally fails faster than LDPE. For a given strain, HDPE's greater modulus causes it to be stressed close to or beyond its yield stress, resulting in failure, whereas LDPE,

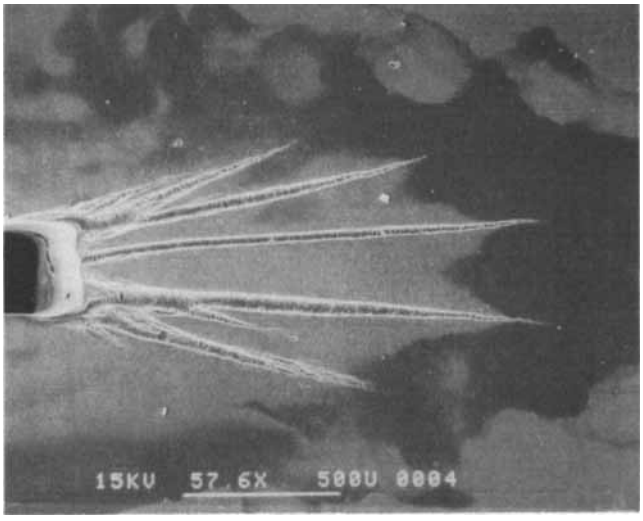

FIGURE 8 Etched interior surface of Marlex 8600 drawn in air.

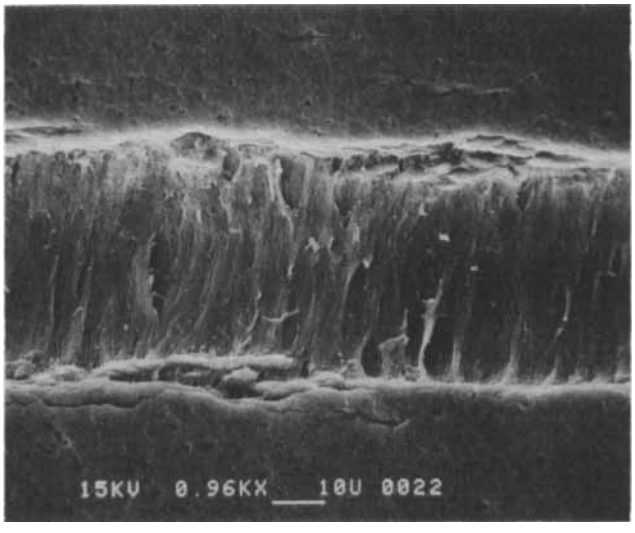

FIGURE 9 Higher magnification SEM micrograph of a Marlex 8600 compact tension specimen pulled in air.

with its lower modulus, is not stressed as close to its yield stress under the same test conditions. Just the reverse occurs in constant stress tests, LDPE samples fail quicker under constant stress because their lower modulus causes them to be stressed close to or beyond their yield stress. In contrast, because of its higher modulus, HDPE is not stressed enough to even approach its yield stress under identical loading conditions. Therefore, neither a constant stress nor a constant strain test is totally suitable for discerning the lifetime of various resins.

With this fundamental problem in the testing of PE resins in mind, it was decided

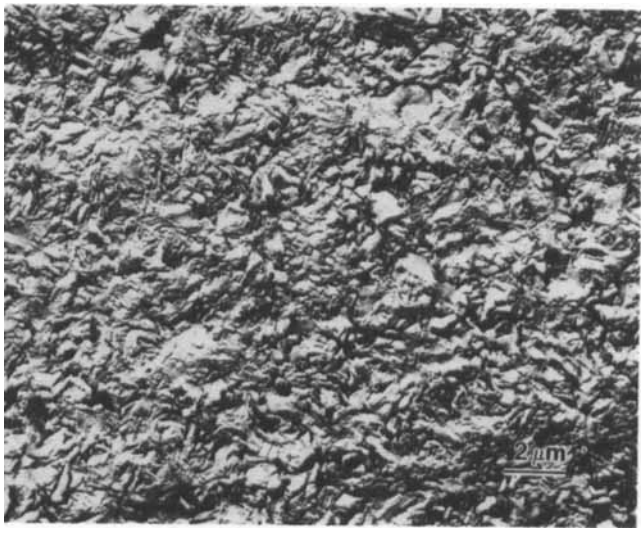

FIGURE 10 TEM micrograph from an undeformed compact tension specimen.

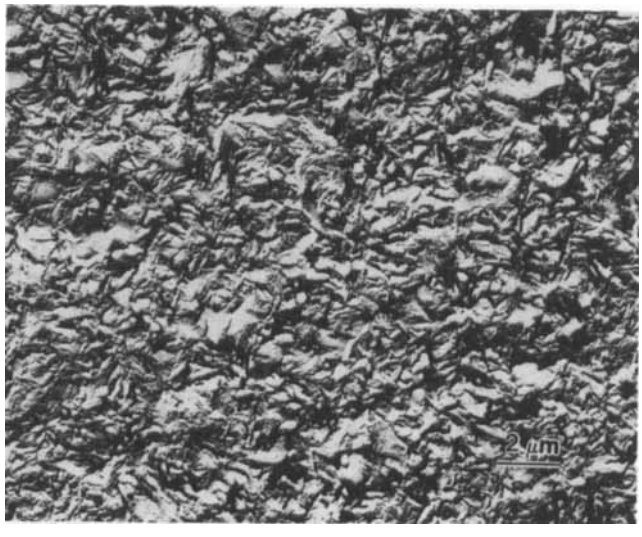

FIGURE 11 TEM micrograph of the region between the craze/crack arms of a compact tension specimen.

to use a compact tension (CT) sample to study changes in morphology occurring during crack growth. The technique used was initially developed in our labs for a similar study of J1 polymer (DuPont).[20] The dimension of the specimen in the direction parallel to the crack front (i.e. the thickness of the specimen used in these studies) has a strong influence on the state of stress which is acting at the crack tip and therefore on the overall observed deformation and toughness. When a sample is thick in the direction parallel to the crack front, a large through-thickness stress can be generated during loading which will restrict the size of the plastic

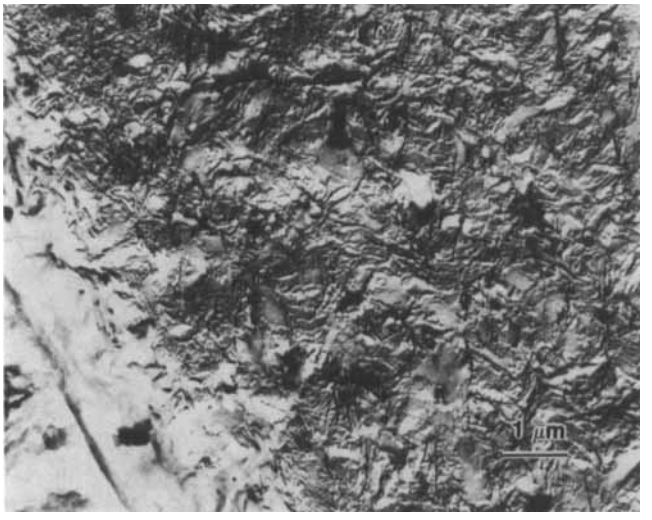

FIGURE 12 TEM micrograph of Marlex 8600 showing the edges of the growing craze.

deformation zone. Because negative stresses in both the thickness and width directions are created, the strain generated in the loading direction is severely restricted. The development of these stresses results in a condition of triaxial stress acting at the crack tip, making void formation more likely because of the constant volume constraint. Testing under these conditions is called plane strain.

When the sample thickness is small, the degree of constraint at the crack tip is minimal and a plane stress condition prevails. A state of biaxial stress rather than triaxial stress exists around the crack tip because, with a thin sample, the through-thickness stress cannot increase appreciably. Because of this phenomenon, properties such as fracture toughness vary with specimen thickness. The fracture toughness of a material depends on the volume of material capable of deforming during fracture and this volume depends on the sample thickness (i.e. deformation zone size). A thinner sample exhibits maximum material toughness while a thicker sample exhibits a lower level of toughness. The fracture toughness will decrease to a constant level as the sample thickness is increased, making this value a conservative lower limit of a material's toughness in any given design application. The thickness of the specimens used in these studies was chosen to be within this region of constant toughness.[21] However, an entire sample is never fully in plane strain, the exterior unbounded surfaces are always in a state of plane stress with the degree of plane strain increasing toward the central regions.

Because it is the crack growth in the interior that is of the most interest, a suitable technique was developed for sectioning the CT specimens in such a manner as to allow characterization of the deformation zone in the interior of the sample. The as-cut surface of a Marlex 400 CT sample drawn in air is shown in Figure 3. In order to obtain better micrographs, etching of the sectioned surface was required to remove the damage caused by the razor blade. Despite the lack of crack advance on the surface of the Marlex 400 samples, all samples showed evidence of interior

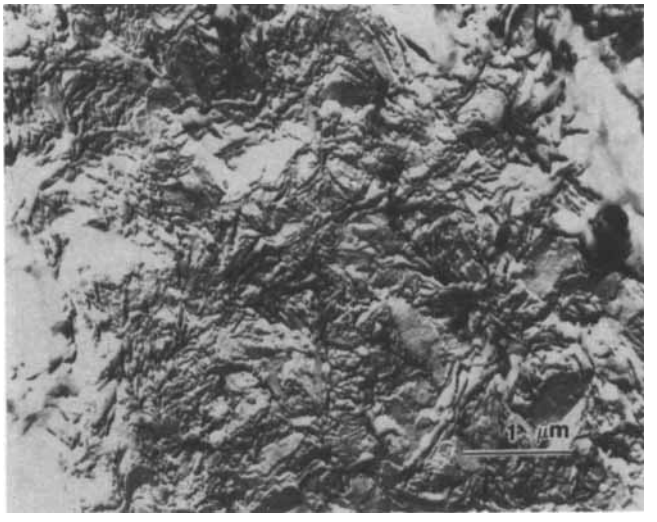

FIGURE 13 TEM micrograph of a region bounded on two sides by crazes in Marlex 8600.

crack development. The multiple cracks initiate at the blunted razor blade crack tip.

Figures 4–7 show various magnifications of an etched Marlex 400 sample with an initial total crack length of 0.308 inch, drawn in air until a COD of 0.1 inch was reached. Three primary crazes/cracks are seen in Figure 4, one in the direction of the "crack advancement" and one on either side at a slight angle. This set of three crazes/cracks allows a considerable amount of energy to be dissipated during failure, retarding the craze/crack growth. It is also noted that the individual craze/cracks, in general, were observed to have a well-defined shape with a width-to-length ratio of less than 0.1 and a sharp boundary delineating the craze and bulk polymer. At SEM magnifications the morphology of the regions surrounding the crack could not be resolved; therefore TEM replication was used to study these regions and will be discussed later in this section.

In Figure 4 two additional effects of major interest are visible; the dark regions surrounding the cracks and the fiber texture within the craze/crack region. In the less drawn region near the tip of the upper side craze/crack the initial formation of large diameter fibrils is evident, as seen in Figure 5. Most of the fibrils form perpendicular to the maximum principal stress direction with the fibril structure being weak in shear. The craze appears to grow longer by a process of fibrillation at the crack tip. In Figure 6, near the base of the central craze/crack, these fibers have been drawn sufficiently to form a smooth surface. In Figure 7, a higher magnification of the base of the craze/crack region, a number of broken fibrils are present. It is not known if this occurred during deformation or etching. Also, it is noted that the fibrillar surface of the crazed/cracked region is significantly below that of the adjoining regions. This could be caused by greater etching of the fibers in the crazed/cracked region due to reduced density or increased surface area.

The origin of the dark areas, which are seen (Figure 4) to extend just beyond the craze/cracks and are not seen in the etched, notched undrawn sample, were

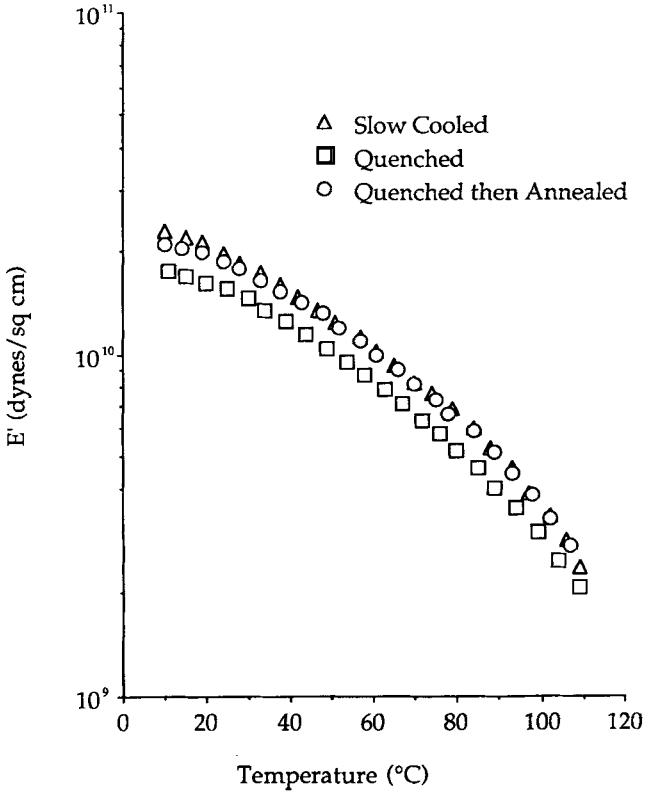

FIGURE 14 Dynamic mechanical spectra E' of Marlex 6050 samples.

investigated by EDAX. The EDAX spectra show the presence of a small amount of phosphorous in the black regions only, which has remained after the etching process. This increased concentration of phosphorous may be due to cavitations resulting from the deformation at the edges of the crazed/cracked region allowing greater retention of the phosphorous in the strained regions than in the unstrained regions.

Several important observations of the craze/crack process were determined from these experiments which were important to the development of the theoretical computer model[4] concurrent with this project; 1) the craze/crack, in general, was observed to have a well-defined shape with a width-to-length ratio of less than 0.1; 2) the boundary that delineates the craze and bulk polymer is sharp; 3) most of the fibrils form perpendicular to the maximum principal stress direction with the fibril structure being weak in shear; and 4) a craze grows by a process of fibrillation at its tip.

Similar SEM studies were conducted to examine the microstructural changes of Marlex 8600 during craze/crack growth in compact tension pieces. This material showed results similar to those observed in Marlex 400. The observations, however, were extended further using TEM techniques to study changes that might be occurring between the crazes.

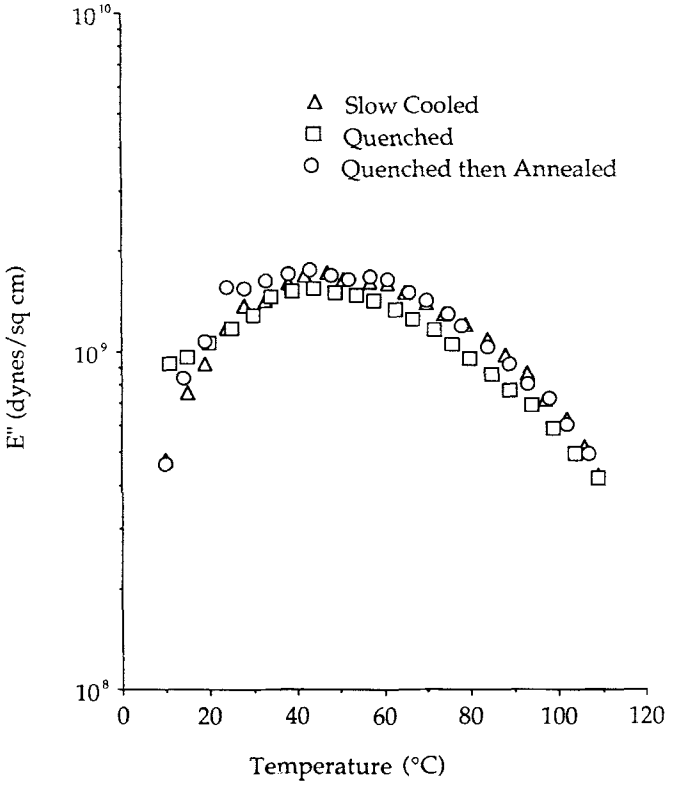

FIGURE 15 Dynamic mechanical spectra E'' of Marlex 6050 samples.

Although there was no visible craze or crack propagation on the exterior surface of this material either, sectioning revealed craze/crack growth on the interior. The as-cut surface was unsuitable for examination as before, so each piece was etched in a 5% solution of $KMnO_4/H_3PO_4$ for 1 hour to reveal the morphology as described earlier. Samples drawn in air showed similar multiple symmetric craze/crack growth when sectioned (Figure 8) except that each outer craze/crack has a side craze/crack. In these samples the dark region incorporates the entire craze/crack region not just the craze/cracks alone. The material within the crazes is uniformly drawn, very coherent in appearance, and almost totally absent of voids, as shown in Figure 9. Also, it is again noted that the fibrillar surface of the crazed/cracked region is significantly below that of the adjoining regions, possibly for the same reasons given before. In summary, even though on the surface no craze/crack growth was seen, internally the initial crack has advanced significantly through crazing.

TEM examination of the material in the region between the craze/crack arms was conducted to determine if and how it is affected by craze-crack growth. Figure 10 is a TEM micrograph of an undeformed compact tension sample sectioned and etched. It shows reasonably well formed lamellae and can serve as an example of undeformed material for comparison with later micrographs. Because of the rough nature of the material within the crazed/cracked region, the replicas held so tightly

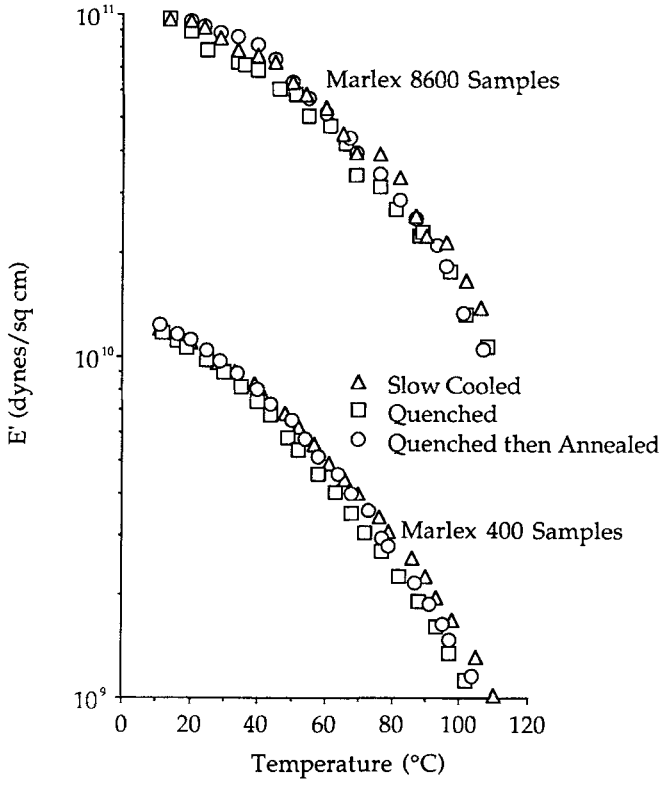

FIGURE 16 Dynamic mechanical spectra E' of Marlex 400 and 8600 samples.

to the polyethylene they could not be pulled off the surface. To overcome this problem, a razor blade was used to cut through the craze arms, freeing the replica and allowing it to be peeled off. Replicas of regions well in front of the growing crazes, showed lamellae similar to those seen in Figure 10. This is as expected, since it is unlikely any deformation has occurred far in front of the growing craze/crack. Figure 11 is a micrograph of a region in between two of the crazes showing lamellae but no sign of drawing or plastic deformation from craze/crack growth, at the resolution of TEM. However, since they would not be observable by TEM, lamella slippage or twinning cannot be ruled out as a possible deformation mechanism; they could account, however, for only a small degree of plastic deformation. This leads us to believe that the majority of the plastic deformation occurring during craze/crack growth is within the crazes and possibly in a thin region close to the edges of the crazes, leaving the regions in between the crazes deformed to a much lesser degree, if any. Because of the razor blade cutting needed to remove the replicas, the area just next to the craze's edge is damaged beyond examination. It is, unfortunately, this region which might be of the most interest.

Several possible methods for examining the region just adjacent to the craze edge were attempted. They all incorporated the general idea of filling the crack with some etch-resistant, low viscosity material that could be hardened and then sectioned. With the crazes filled it was believed the TEM replicas could be removed

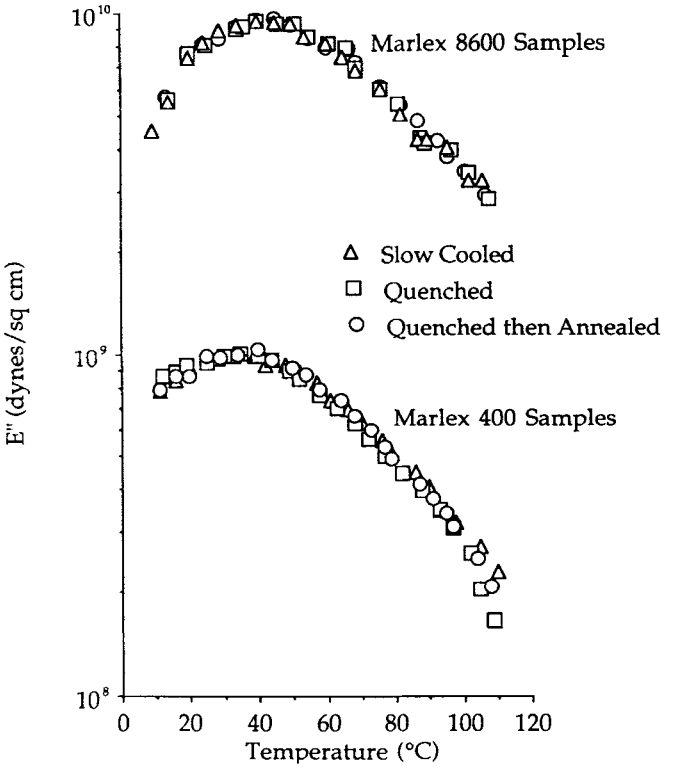

FIGURE 17 Dynamic mechanical spectra E'' of Marlex 400 and 8600 samples.

easily. (It was the roughness and voids of the crazes that allowed the replica to adhere so strongly that it could not be removed.) CT specimens, molded and deformed as described earlier, were used. Five minute epoxy, styrene monomer (later polymerized in place) and wax were chosen as possible mediums. Of the three, only wax was found to be suitable. Because of the initial crack's small opening and the coherent nature of the craze, none of the material would flow into the crazed region. Thus, the CT piece was placed in molten wax (the wax melted at 55°C) and a vacuum was drawn on the molten wax and CT piece. After the piece had been in the vacuum for 30 minutes it was removed, cooled, sectioned and etched as described for the other experiments. Figure 12 is a TEM micrograph of Marlex 8600 with a craze running through it. The wax is at the left hand side of the picture running on an angle. The region where the picture's texture changes is the edge of the craze/crack and further to the right is the material between the crazes. This region shows no observable deformation. Thus, it is concluded that most of the deformation generated during craze growth is confined to the region within the crazes rather than the region between the crazes. Figure 13 is a micrograph of a small region bordered by two growing crazes/cracks (upper right and lower left corners). Even a region such as this, which would be expected to be under great stress during craze/crack growth, shows no observable deformation,

confirming our belief that the majority of the deformation process is confined to within and at the very edge of the crazed region.

Molecular mobility and its effect on crack growth

Dynamic mechanical measurements were made on both Marlex 400 and 8600 as well as Marlex 6050; the latter is a HDPE containing almost no branches. Thin sheets (0.029" thick) were slow cooled or quenched from the melt in the press after compression molding at 165°C for 15 minutes. Annealing was done, when desired, at 110°C for 12 hours under vacuum. This is 15°C below the melting point of the pipe resins (~125°C). Figures 14 and 15 show E' and E'' for the HDPE. Since the slow cooled sample is expected to be more crystalline, on average, than the quenched specimen, its modulus is greater over the entire temperature range measured, as seen in Figure 14. For the slow cooled specimen the α-relaxation peak (Figure 15), corresponding to motion in crystalline regions, is greater than that of the quenched specimen over the entire temperature range, as expected. Annealing a quenched sample at 110°C for 12 hours causes its dynamic mechanical spectra to resemble that of the slow cooled sample, with a maximum at about 50°C. This demonstrates that molecular motion within the crystals of LPE Marlex 6050 is possible to a reasonable degree and that the rate of cooling can influence crystallinity.

The spectra of the slow cooled and annealed specimens closely resemble those obtained by Takayanagi and Matsuo, at 11 cps, of single crystals annealed at 90°C; both α_c' and α_c can be seen, at ca. 45 and 60°C. Since our frequency (1 cps) was lower, the two peaks would be expected at lower temperatures; at 11 cps, a sample crystallized at 70°C had peaks at ca. 35 and 50°C. Unfortunately they did not examine the effect of crystallization rate and annealing for their bulk specimens. α_f is not seen for these samples; it was seen clearly by Takayanagi and Matsuo only for single crystals grown isothermally at temperatures below 70°C, i.e. with

TABLE II

Percent crystallinities of various PE resins with different thermal histories as determined by WAXS and DSC

	WAXS	DSC
Marlex 400		
Slow Cooled	56.2	53.5
Quenched	58.2	54.1
Quenched/Annealed	57.7	53.8
Marlex 6050		
Slow Cooled	69.4	82.9
Quenched	64.5	72.8
Quenched/Annealed	70.7	81.0
Marlex 8600		
Slow Cooled	57.0	56.5
Quenched	57.1	56.5
Quenched/Annealed	57.3	57.4

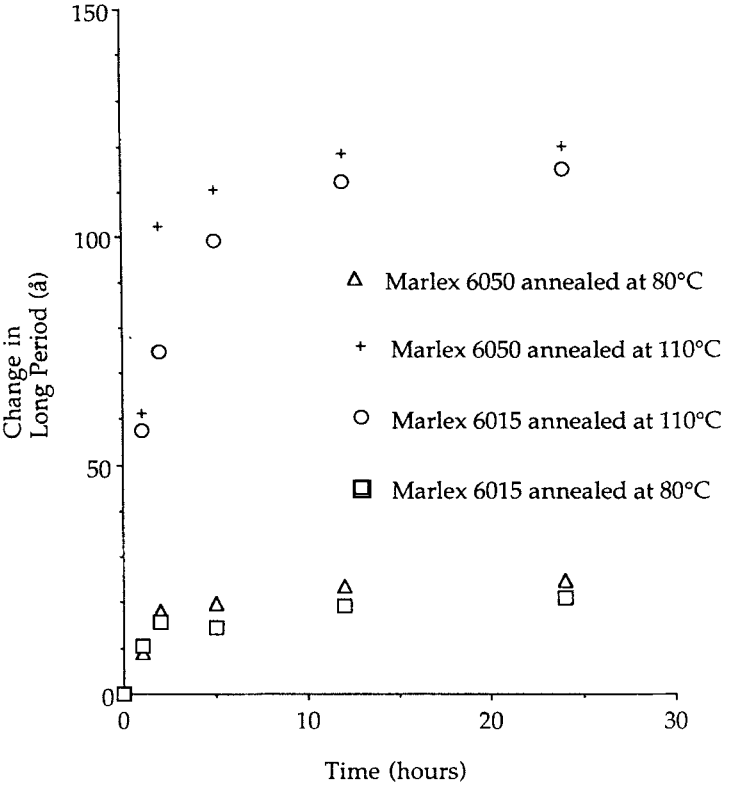

FIGURE 18 Change in long period versus annealing time and temperature for Marlex 6050 and 6015.

lamellae less than 115Å thick; α_f increases in temperature with increasing lamellar thickness. Our 6050 samples had SAXS long periods of 265Å and 384Å for the quenched, and quenched, annealed samples, respectively.

Contrary to the HDPE spectra, there was no distinguishable difference between the dynamic mechanical spectra (Figures 16 and 17) of samples with various thermal history from the two pipe resins, Marlex 400 and 8600, which were tested. Only a single peak is seen, as reported by Takayanagi and Matsuo for single crystals which have undergone lamellar thickening. This suggests the possiblity that branch content, rather than cooling rate or annealing, is the primary factor controlling crystallization and morphology in the pipe resins. Because these branches are excluded from the crystalline regions during crystallization,[22] difficulties in both initial lamella formation and motion of the molecules in the lamellae during annealing of these pipe resins are expected. These difficulties due to branch content are far less apparent or are absent in polyethylenes such as Marlex 6050, as might be expected. It is just this reduced molecular motion of the polymer chains in the pipe resins lamellae which we suggest may play a significant role during crack growth by resisting chain slippage of tie molecules.

DSC and WAXS results (Table II) from the actual samples tested in the Rheometrics tend to confirm the above suggestions. Although the absolute values be-

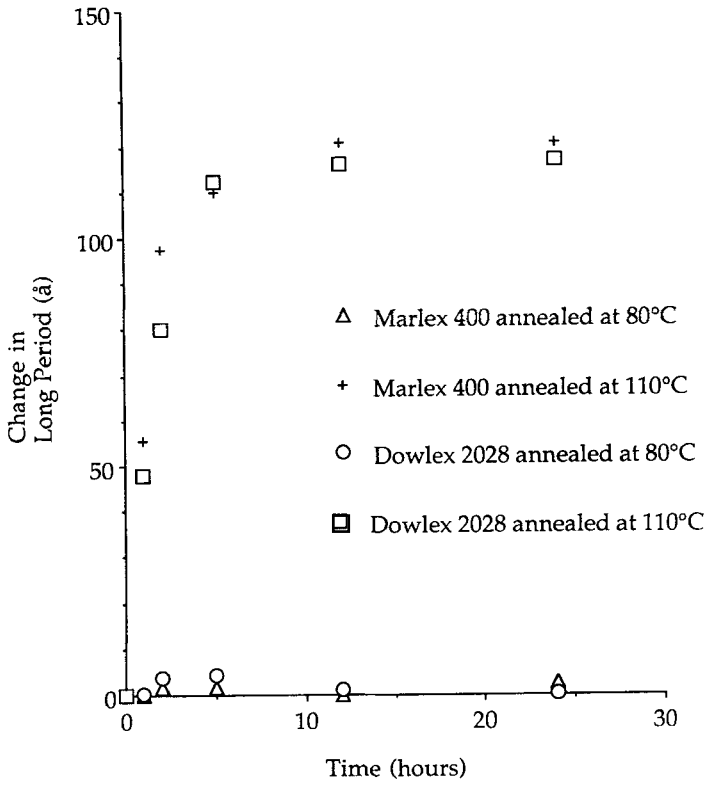

FIGURE 19 Change in long period versus annealing time and temperature for Marlex 400 and Dowlex 2028.

tween the two methods vary, the trends are identical. Marlex 400 and 8600 show no change in crystallinity with respect to thermal history, whereas Marlex 6050 shows higher crystallinity in slow cooled samples and an increase in crystallinity after annealing.

SAXS studies also confirmed the difficulty of molecular motion in the gas pipe resins, which we attribute to branch length and number. Samples 0.010 of an inch thick were molded and quenched in ice water immediately after pressing in order to create the smallest possible lamella thickness. The change in long period versus time and versus temperature of annealing were measured to give an indication of chain mobility within the crystalline regions. Chains with reduced mobility (i.e. those containing side branches) will require more annealing time or higher annealing temperatures to achieve comparable thickening of the lamella structure relative to that in linear polymers. Marlex 8600 could not be used in these studies because the only available samples of this resin contained carbon black. The carbon particles in the 8600 resin scatter so intensely that the scattering from the crystalline regions is obscured making measurements of the long period impossible.

Two annealing temperatures were used, 80 and 110°C, and several PE's of various branch length were tested. Figure 18 shows the results from two HDPE resins Marlex 6015 and 6050; notice that the change in long period is slightly greater for

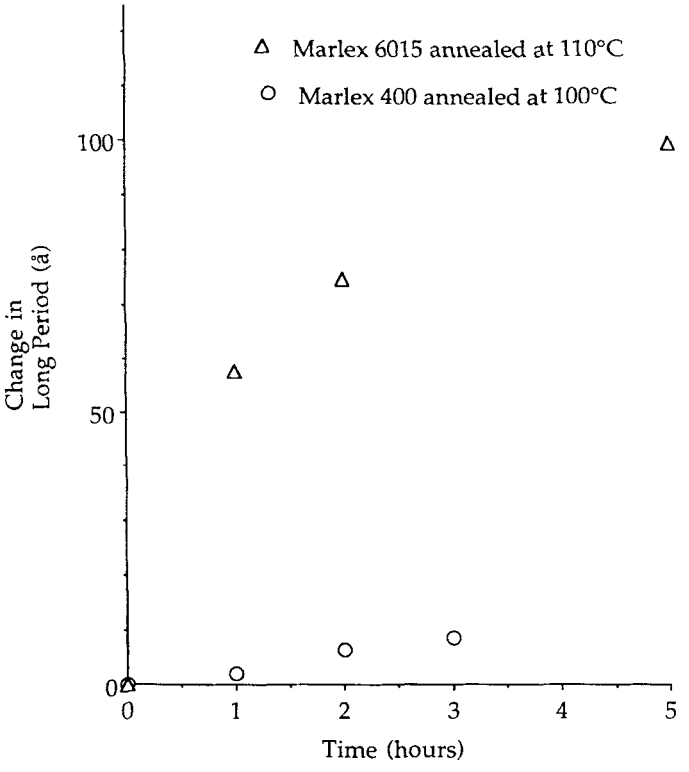

FIGURE 20 Change in long period versus annealing time for Marlex 400 and 6015 at the same degree of super cooling.

the Marlex 6050 sample than the Marlex 6015 sample at any given time, probably due to the higher molecular weight of Marlex 6015. Both figures show large increases in the long period when annealed at 110°C, as expected. When annealed at 80°C a slight increase in long period is seen, demonstrating that chain motion through the crystalline regions is still possible in these quenched samples even at this low temperature. When two resins with branches were tested, Marlex 400 with a butyl branch and Dowlex 2028 with an even longer hexyl branch (Figure 19), essentially the same long period increases were seen in samples annealed at 110°C as for the HDPE samples. The increase in long period of Dowlex 2028 is slightly less than that of the Marlex 400, possibly because of its longer side branch. Annealing at 80°C, however, showed no increase in the long period for either branched resin.

In order to make a direct comparison of the HDPE results with those of the pipe resins, an adjustment should be made in their respective annealing temperature which accounts for the differences in their melting points. Marlex 400 melts ten degrees lower than Marlex 6015. Figure 20 is a plot of the change in the long period versus time for Marlex 6015 annealed at 110°C and Marlex 400 annealed at 100°C; clearly the long period change in the gas pipe resin is significantly less. We attribute reduced chain mobility within the crystalline regions of the Marlex 400 to the

number and length of the comonomer α-olefin since there is little difference between the melt indexes of these two materials.

CONCLUSIONS

The objective of this study was to develop a fundamental understanding of crack growth in polyethylene copolymers used in the natural gas industry as distribution piping. Although these materials have a very low comonomer concentration, its effect is significant. Compact tension specimens showed several significant features of the crack growth process. Although a single crack was used for initiation, this crack quickly divided into three or five symmetric crazes with a well defined shape and a thickness to width ratio of less than 0.1. The growth of the craze is by a process of fibrillation at the crack tip, with most of the fibrils formed perpendicular to the maximum principal stress. The molecular mobility of these materials was determined from their dynamic mechanical properties and from small angle x-ray scattering measurements of the change in long period with annealing time and temperature. These studies showed that molecular mobility in these gas pipe resins is significantly less than that seen in HDPE. This greatly reduced molecular mobility is believed to be partially responsible for the increased resistance to slow crack growth of these resins. In subsequent papers we examine the effect of ESC agents, the presence of a second, rubbery phase and variations in morphology through the pipe wall thickness on the crack growth process.

Acknowledgments

This research was supported by the Gas Research Institute. Appreciation is expressed to S. S. Wang, F. G. Yuan and A. Miyase, University of Illinois and M. Klein, Gas Research Institute for helpful discussions.

References

1. A. Lustiger, J. Cassady, F. S. Uralil and L. E. Hulbert, Field Failure Reference Catalog for Polyethylene Gas Piping, Gas Research Institute GRI 84/023511, 1984.
2. J. Watts, *Pipeline and Gas Journal*, **14,** 19 (1982).
3. National Transportation Safety Board (NTSB), An Analysis of Accident Data from Plastic Pipe Natural Gas Distribution Systems, Technical Report No. PSS-80-1, 1980.
4. F. G. Yuan and S. S. Wang, Gas Research Institute GRI-88/0221 (1988).
5. A. Lustiger and R. D. Corneliussen, *Mod. Plast.*, **3,** 74 (1986).
6. I. L. Hopkins, W. D. Baker and J. B. Howard, *J. Appl. Phys.*, **21,** 207 (1959).
7. J. B. Howard, *J. Soc. Plast. Eng.*, **15,** 397 (1959).
8. C. G. Bragaw, *Polym. Plast. Proc. Appl.*, **1,** 145 (1979).
9. S. Bandopapadhykay and H. R. Brown, *Polym.*, **22,** 245 (1981).
10. K. Richards, *Plastics*, **12,** 444 (1958).
11. M. Takayanagi and T. Matsuo, *J. Macromol. Sci., Phys.*, **B1**, 407 (1967).
12. R. H. Olley, A. M. Hodge and D. C. Bassett, *J. Polym. Sci., Polym. Phys. Ed.*, **17,** 627 (1979).
13. F. Rybnikar, *J. Appl. Poly. Sci.*, **30,** 1949 (1985).
14. F. W. Billmeyer, *J. Appl. Phys.*, **28,** 1114 (1957).
15. N. Brown and S. K. Bhattacharya, *J. Matr'l. Sci.*, **20,** 4553 (1985).

16. X. Lu and N. Brown, *J. Matr'l. Sci.*, **21,** 2423 (1986).
17. R. A. Bubeck, *Polym.*, **22,** 683 (1981).
18. R. A. Bubeck and H. M. Baker, *Polym.*, **23,** 1680 (1982).
19. A. Lustiger and R. D. Corneliussen, *J. Matr'l. Sci.*, **22,** 2470 (1987).
20. A. Chen, Ph.D. Thesis, Univ. Illinois (1987).
21. S. H. Carr and B. Crist, Gas Research Institute Annual Report, GRI 87/0039, (September, 1985–August, 1986).
22. P. D. Frayer, P. Po-Luk Tong and W. W. Dreher, *Polym. Eng. Sci.*, **17,** 27 (1977).